Chemistry of *C*-Trimethylsilyl-Substituted Heterocarboranes. 14. Syntheses of *closo*-Indacarboranes and Their Reactivity toward a Bis(bidentate) Lewis Base, 2,2′-Bipyrimidine: Crystal Structures of *closo*-1-(Me_2CH)-1-In-2,3-($SiMe_3$)$_2$-2,3-$C_2B_4H_4$ and 1-(2,2′-$C_8H_6N_4$)-1-(Me_2CH)-1-In-2,3-($SiMe_3$)$_2$-2,3-$C_2B_4H_4$[§]

Narayan S. Hosmane,*[†] Kai-Juan Lu,[†] Anil K. Saxena,[†] Hongming Zhang,[†] John A. Maguire,[†] Alan H. Cowley,[‡] and Rodney D. Schluter[‡]

Departments of Chemistry, Southern Methodist University, Dallas, Texas 75275, and University of Texas at Austin, Austin, Texas 78712

Received July 13, 1993[®]

The reaction of (*i*-Pr)InI_2 with the THF-solvated sodium lithium compounds *closo-exo*-4,5-Li(THF)-1-Na(THF)-2-($SiMe_3$)-3-R-2,3-$C_2B_4H_4$ (R = $SiMe_3$, Me, H) in a molar ratio of 1:1 in THF produced *closo*-1-(Me_2CH)-1-In-2,3-($SiMe_3$)$_2$-2,3-$C_2B_4H_4$ (**I**), *closo*-1-(Me_2CH)-1-In-2-($SiMe_3$)-3-Me-2,3-$C_2B_4H_4$ (**II**), and *closo*-1-(Me_2CH)-1-In-2-($SiMe_3$)-2,3-$C_2B_4H_5$ (**III**) as air-sensitive colorless oily liquids, in 39, 36, and 27% yields, respectively. The *closo*-indacarboranes **I–III** were characterized on the basis of ^1H, ^{11}B, and ^{13}C pulse Fourier transform NMR and IR spectra. Compound **I** was further characterized by mass spectrometry and X-ray diffraction. The low-temperature, single-crystal X-ray analysis of **I** shows that the indacarborane is a dimeric cluster having a distorted *closo* geometry in which the indium atom occupies an apical vertex of a pentagonal bipyramid and is slipped significantly toward the unique boron above the C_2B_3 face. The indium-bound isopropyl moiety is tilted, with the angle between the In–(*i*-Pr) bond and the normal from the C_2B_3 plane through the In atom being equal to 30.3 ± 1.3°. The *closo*-indacarborane **I** crystallized in the triclinic space group $P\bar{1}$ with a = 11.018(3) Å, b = 12.394(3) Å, c = 14.485(4) Å, α = 73.01(2)°, β = 87.67(2)°, γ = 89.90(2)°, V = 1890.0(9) Å^3, and Z = 2. Full-matrix least-squares refinement of **I** converged at R = 0.027 and R_w = 0.037. The instantaneous reactions between the *closo*-indacarboranes and 2,2′-bipyrimidine produced the donor–acceptor complexes 1-(2,2′-$C_8H_6N_4$)-1-(Me_2CH)-1-In-2,3-($SiMe_3$)$_2$-2,3-$C_2B_4H_4$ (**IV**), 1-(2,2′-$C_8H_6N_4$)-1-(Me_2CH)-1-In-2-($SiMe_3$)-3-Me-2,3-$C_2B_4H_4$ (**V**), and 1-(2,2′-$C_8H_6N_4$)-1-(Me_2CH)-1-In-2-($SiMe_3$)-2,3-$C_2B_4H_5$ (**VI**) in 68–91% yields. The complexes **IV–VI** were all characterized by ^1H, ^{11}B, and ^{13}C NMR and IR spectra. Compound **V** was also characterized by mass spectrometry and **IV** by single-crystal X-ray analysis. It crystallized in the monoclinic space group $P2_1$ with a = 11.428(3) Å, b = 9.802(3) Å, c = 11.972(3) Å, β = 96.28(2)°, V = 1333.0(6) Å^3, and Z = 2. Full-matrix least-squares refinement of **IV** converged at R = 0.026 and R_w = 0.034. The bonding in these complexes was discussed using molecular orbital theory.

Introduction

Since the first report of a synthesis incorporating a main-group metal into a carborane cage,[1] the metallacarboranes have been the subject of a number of investigations.[2] The metallacarboranes of the group 14 elements have been synthesized,[3] and examples of structurally characterized stanna-, germa-, and plumbacarboranes, and their acid–base adducts, are known.[4–8] However, information concerning the carborane derivatives of group 13 metals is much less complete. The aluminacarboranes have been the most extensively investigated organometallics of this group.[2,9] Icosahedral *commo*- and *closo*-aluminacarboranes have been characterized spectroscopically, and a number of structures have been reported.[9] In addition to their intrinsic interest, these aluminacarboranes can also function as useful dicarbollyl transfer agents when treated

† Southern Methodist University.

‡ University of Texas at Austin.

§ Dedicated to Professor M. F. Hawthorne of UCLA on the occasion of his 65th birthday.

® Abstract published in *Advance ACS Abstracts*, February 15, 1994.

(1) (a) Mikhailov, B. M.; Potapova, T. V. *Izv. Akad. Nauk SSSR, Ser. Khim.* **1968**, *5*, 1153. (b) Popp, G.; Hawthorne, M. F. *J. Am. Chem. Soc.* **1968**, *90*, 6553.

(2) (a) Grimes, R. N. In *Comprehensive Organometallic Chemistry*; Wilkinson, G., Stone, F. G. A., Abel, E. W., Eds.; Pergamon: Oxford, U.K., 1982; Vol. 1, Chapter 5.5. (b) Hosmane, N. S.; Maguire, J. A. In *Advances in Boron and the Boranes*; Molecular Structure and Energetics 5; Liebman, J. F., Greenberg, A., Williams, R. E., Eds.; VCH: New York, 1988; Chapter 14, p. 297. (c) Hosmane, N. S.; Maguire, J. A. *Adv. Organomet. Chem.* **1990**, *30*, 99.

(3) (a) Wong, K.-S.; Grimes, R. N. *Inorg. Chem.* **1977**, *16*, 3094. (b) Rudolph, R. W.; Voorhees, R. L.; Cochoy, R. E. *J. Am. Chem. Soc.* **1970**, *92*, 3351.

(4) (a) Hosmane, N. S.; Fagner, J. S.; Zhu, H.; Siriwardane, U.; Maguire, J. A.; Zhang, G.; Pinkston, B. S. *Organometallics* **1989**, *8*, 1769 and references therein. (b) Cowley, A. H.; Galow, P.; Hosmane, N. S.; Jutzi, P.; Norman, N. C. *J. Chem. Soc., Chem. Commun.* **1984**, 1564. (c) Jutzi, P.; Galow, P.; Abu-Orabi, S.; Arif, A. M.; Cowley, A. H.; Norman, N. C. *Organometallics* **1987**, *6*, 1024.

(5) (a) Hosmane, N. S.; de Meester, P.; Maldar, N. N.; Potts, S. B.; Chu, S. S. C.; Herber, R. H. *Organometallics* **1986**, *5*, 772. (b) Hosmane, N. S.; Islam, M. S.; Pinkston, B. S.; Siriwadane, U.; Banewicz, J. J.; Maguire, J. A. *Organometallics* **1988**, *7*, 2340.

(6) Hosmane, N. S.; Lu, K.-J.; Zhang, H.; Maguire, J. A.; Jia, L.; Barreto, R. D. *Organometallics* **1992**, *11*, 2458.

(7) Hosmane, N. S.; Lu, K.-J.; Zhu, H.; Siriwardane, U.; Shet, M. S.; Maguire, J. A. *Organometallics* **1990**, *9*, 808.

(8) Hosmane, N. S.; Lu, K.-J.; Siriwardane, U.; Shet, M. S. *Organometallics* **1990**, *9*, 2798.

(9) Schubert, D. M.; Bandman, M. A.; Rees, W. S., Jr.; Knobler, C. B.; Lu, P.; Nam, W.; Hawthorne, M. F. *Organometallics* **1990**, *9*, 2046 and references therein.

0276-7333/94/2313-0979$04.50/0

with other main-group halides.[10] While aluminacarboranes of small cage systems have been synthesized,[11] they have not been structurally characterized. Structural information concerning the gallacarboranes is fairly sketchy; in the icosahedral system both *closo*- and *commo*-gallacarboranes have been reported, but only the latter ones have been structurally characterized.[9,12] In the pentagonal-bipyramidal system, no *commo*-gallacarboranes are known, but several *closo*-gallacarboranes have been synthesized and structurally characterized.[13–15] On the other hand, there is very little information on the indacarboranes. While there has been a great deal of interest in the π-complexes of indium, they have dealt mainly with In(I) compounds,[16–18] and In(III) complexes, especially with carboranes, have received scant attention.[19–21] A *closo* structure of 1,2,3-$InC_2B_4H_6$ was deduced by Grimes and co-workers from NMR data;[13] however, the other group 13 metallacarboranes all show structural distortions which are not apparent in such data and structure determinations are needed to study the geometries of the metallacarboranes. The only structural characterization of an indacarborane was presented in our preliminary report on 1-(Me_2CH)-1-In^{III}-2,3-$(SiMe_3)_2$-2,3-$C_2B_4H_4$.[21] In addition, there are no studies of the reaction chemistry of the indacarboranes to complement those of the earlier group 13[9–11] and group 14[4–8] metallacarboranes.

In the present paper we describe the details of the preparation, characterization, and properties of *C*-trimethylsilyl-substituted *closo*-indacarboranes and their reactions with 2,2′-bipyrimidine. We also report the X-ray crystal structures of *closo*-1-(Me_2CH)-1-In-2,3-$(SiMe_3)_2$-2,3-$C_2B_4H_4$ (I) and its donor–acceptor complex 1,1′-(2,2′-$C_8H_6N_4$)-1-(Me_2CH)-1-In-2,3-$(SiMe_3)_2$-2,3-$C_2B_4H_4$ (**IV**), along with a molecular orbital analysis of these compounds.

Experimental Section

Materials. 2,3-Bis(trimethylsilyl)-2,3-dicarba-*nido*-hexaborane(8), 2-(trimethylsilyl)-3-methyl-2,3-dicarba-*nido*-hexaborane(8), and 2-(trimethylsilyl)-2,3-dicarba-*nido*-hexaborane(8) were prepared by the methods of Hosmane *et al.*[22–25] Solutions of *closo-exo*-4,5-Li(THF)-1-Na(THF)-2-$(SiMe_3)$-3-R-2,3-$C_2B_4H_4$ (R = $SiMe_3$, Me, H) in tetrahydrofuran (THF) were prepared by the method described earlier.[26] (*i*-Pr)InI_2 was prepared and purified according to the literature method.[27] Prior to use, 2,2′-bipyrimidne (Lancaster Syntheses, Windham, NH) was sublimed *in vacuo*, and its purity was checked by IR, NMR, and melting point measurements. Benzene, tetrahydrofuran (THF), and *n*-hexane were dried over $LiAlH_4$ and doubly distilled before use. All other solvents were dried over 4–8 mesh molecular sieves (Aldrich) and either saturated with dry argon or degassed. Immediately before use, NaH (Aldrich), in a mineral oil dispersion, was washed repeatedly with dry *n*-pentane. *tert*-Butyllithium, *t*-BuLi (1.7 M solution in pentane, Aldrich), was used as received.

Spectroscopic and Analytical Procedures. Proton, boron-11, and carbon-13 pulse Fourier transform NMR spectra, at 200, 64.2 and 50.3 MHz, respectively, were recorded on an IBM WP200 SY multinuclear NMR spectrometer. Infrared spectra were recorded on a Perkin-Elmer Model 283 infrared spectrophotometer and a Perkin-Elmer Model 1600 FT-IR spectrophotometer. Elemental analyses were obtained from E+R Microanalytical Laboratory, Inc., Corona, NY. Mass spectral determinations were performed by the Midwest Center for Mass Spectrometry, University of Nebraska—Lincoln, Lincoln, NE.

Synthetic Procedures. All experiments were carried out in Pyrex glass round-bottom flasks of 250-mL capacity, containing magnetic stirring bars and fitted with high-vacuum Teflon valves. Nonvolatile substances were manipulated in either a drybox or evacuable glovebags under an atmosphere of dry nitrogen. All known compounds among the products were identified by comparing their IR and NMR spectra with those of the authentic samples.

Synthesis of *closo*-1-(Me_2CH)-1-In-2-$(SiMe_3)$-3-R-2,3-$C_2B_4H_4$ (R = Me_3Si, Me, H). A THF solution (15 mL) containing 3.323 g (8.48 mmol), 1.214 g (3.64 mmol), or 1.329 g (4.16 mmol) of *closo-exo*-4,5-Li(THF)-1-Na(THF)-2-$(SiMe_3)$-3-R-2,3-$C_2B_4H_4$ (R = $SiMe_3$, Me, H) was poured slowly *in vacuo* onto the THF solution (10 mL) of freshly prepared, anhydrous (*i*-Pr)InI_2 (3.49 g, 8.493 mmol; 1.50 g, 3.64 mmol; 1.72 g, 4.16 mmol) at −23 °C, and the mixture was stirred constantly for 2 h. After removal of THF at this temperature via vacuum distillation, the reaction flask, containing an off-white residue, was attached to a detachable high-vacuum U-trap which was immersed in a dry-ice/2-propanol bath. With fractional distillation and/or sublimation procedures, temperatures, and times identical with those described for the syntheses of *closo*-galla- and *closo*-germacarborane derivatives,[5b,14] the off-white residue gave the corresponding *closo*-indacarborane product in the U-trap. The impure indacarborane was then heated to 50 °C and was slowly fractionated (24 h) through U-traps held at room temperature (cool water bath) and 0 and −78 °C, respectively, to collect *closo*-1-(Me_2CH)-1-In-2,3-$(SiMe_3)_2$-2,3-$C_2B_4H_4$ (**I**) (1.25 g, 3.32 mmol; 39% yield), *closo*-1-(Me_2CH)-1-In-2-$(SiMe_3)$-3-Me-2,3-$C_2B_4H_4$ (**II**) (0.41 g, 1.31 mmol; 36% yield), or *closo*-1-(Me_2CH)-1-In-2-$(SiMe_3)$-2,3-$C_2B_4H_5$ (**III**) (0.347 g, 1.14 mmol; 27% yield) in the room-temperature trap. Some of the corresponding neutral *nido*-carborane precursor 2-$(SiMe_3)$-3-R-2,3-$C_2B_4H_6$ (3–4 mmol) was also recovered in the −78 °C trap; no material collected in the 0 °C trap.

All these complexes melt at, or slightly below, room temperature to give colorless oily liquids (bp under high vacuum (10^{-4} Torr): **I**, 135 °C; **II**, 148 °C; **III**, 127 °C). Compound **I** had the highest melting point and was crystalline at room temperature; depending on the local temperature, the other compounds would melt, or solidify, during workups, making them especially difficult to handle and purify. The complexes are highly soluble in both polar and nonpolar organic solvents. Crystals of compound **I** were directly sent for elemental and mass spectral analysis, while compounds **II** and **III** were dissolved in C_6H_6 and transferred to sample vials and then the C_6H_6 was removed by pumping under high vacuum for 12 h. Mass spectral analysis (high-

(10) Jutzi, P.; Galow, P. *J. Organomet. Chem.* **1987**, *319*, 139.
(11) (a) Magee, C. P.; Sneddon, L. G.; Beer, D. C.; Grimes, R. N. *J. Organomet. Chem.* **1975**, *86*, 159. (b) Beck, J. S.; Sneddon, L. G. *J. Am. Chem. Soc.* **1988**, *110*, 3467.
(12) Bandman, M. A.; Knobler, C. B.; Hawthorne, M. F. *Inorg. Chem.* **1989**, *28*, 1204.
(13) Grimes, R. N.; Rademaker, W. J.; Denniston, M. L.; Bryan, R. F.; Greene, P. T. *J. Am. Chem. Soc.* **1972**, *94*, 1865.
(14) Hosmane, N. S.; Lu, K.-J.; Zhang, H.; Jia, L.; Cowley, A. H.; Mardones, M. A. *Organometallics* **1991**, *10*, 963.
(15) Hosmane, N. S.; Zhang, H.; Lu, K.-J.; Maguire, J. A.; Cowley, A. H.; Mardones, M. A. *Struct. Chem.* **1992**, *3*, 183.
(16) Janiak, C.; Hoffman, R. *J. Am. Chem. Soc.* **1990**, *112*, 5924.
(17) (a) Beachley, O. T., Jr.; Lees, J. F.; Glassman, T. E.; Churchill, M. R.; Buttrey, L. A. *Organometallics* **1990**, *9*, 2488 and references therein. (b) Manning, M. J.; Knobler, C. B.; Hawthorne, M. F.; Do, Y. *Inorg. Chem.* **1991**, *30*, 3589.
(18) Schumann, H.; Janiak, C.; Gorlitz, F.; Loebel, J.; Dietrich, A. *J. Organomet. Chem.* **1989**, *363*, 243.
(19) See ref 13 for the synthesis of 1-$CH_3InC_2B_4H_6$.
(20) Greenwood, N. N.; Thomas, B. S.; Waite, D. W. *J. Chem. Soc., Dalton Trans.* **1975**, 299.
(21) Hosmane, N. S.; Lu, K.-J.; Zhang, H.; Cowley, A. H.; Mardones, M. A. *Organometallics* **1991**, *10*, 392.
(22) Hosmane, N. S.; Sirmokadam, N. N.; Mollenhauer, M. N. *J. Organomet. Chem.* **1985**, *279*, 359.
(23) Hosmane, N. S.; Mollenhauer, M. N.; Cowley, A. H.; Norman, N. C. *Organometallics* **1985**, *4*, 194.
(24) Hosmane, N. S.; Maldar, N. N.; Potts, S. B.; Rankin, D. W. H.; Robertson, H. E. *Inorg. Chem.* **1986**, *25*, 1561.
(25) Hosmane, N. S.; Islam, M. S.; Burns, E. G. *Inorg. Chem.* **1987**, *26*, 3236.
(26) Hosmane, N. S.; Barreto, R. D. *Inorg. Synth.* **1992**, *29*, 295.
(27) Hoffman, G. G.; Faist, R. *J. Organomet. Chem.* **1990**, *391*, 1.

resolution electron impact (HREI) peak match): theoretical mass for I, $^{12}C_{11}{}^{1}H_{29}{}^{10}B^{11}B_3{}^{28}Si_2{}^{115}In$, and $^{12}C_{11}{}^{1}H_{29}{}^{11}B_4{}^{28}Si_2{}^{115}In$ m/e 375.1255 and 376.1219, measured mass m/e 375.1259 and 376.1229. Anal. Calcd for $C_{11}H_{29}B_4Si_2In$ (I): C, 35.12; H, 7.71. Found: C, 35.27; H, 7.32. Calcd for $C_9H_{23}B_4SiIn{\cdot}2C_6H_6$ (II): C, 53.27; H, 7.39. Found: C, 55.75; H, 9.71. Calcd for $C_8H_{21}B_4SiIn{\cdot}C_6H_6$ (III): C, 41.67; H, 7.07. Found: 41.67; H, 7.67.

Synthesis of 1-(2,2′-$C_8H_6N_4$)-1-(Me_2CH)-1-In-2-($SiMe_3$)-3-R-2,3-$C_2B_4H_4$ (R = $SiMe_3$, Me, H). In a procedure similar to that employed for the synthesis of donor–acceptor complexes involving 2,2′-bipyrimidine and *closo*-galla- and *closo*-stannacarboranes, described elsewhere,[3,14,15] 1.25 mmol (0.47 g) of *closo*-1-(Me_2CH)-1-In-2,3-($SiMe_3$)$_2$-2,3-$C_2B_4H_4$ (I), 2.71 mmol (0.86 g) of *closo*-1-(Me_2CH)-1-In-2-($SiMe_3$)-3-Me-2,3-$C_2B_4H_4$ (II), or 1.91 mmol (0.58 g) of *closo*-1-(Me_2CH)-1-In-2-($SiMe_3$)-2,3-$C_2B_4H_5$ (III) was treated with freshly sublimed, anhydrous 2,2′-bipyrimidine, $C_8H_6N_4$ (0.099 g, 0.625 mmol; 0.215 g, 1.36 mmol; 0.152 g, 0.96 mmol) in dry benzene at room temperature for 4 h. This resulted in the isolation of red crystals of 1-(2,2′-$C_8H_6N_4$)-1-(Me_2CH)-1-In-2,3-($SiMe_3$)$_2$-2,3-$C_2B_4H_4$ (IV) (0.307 g, 0.57 mmol; 91% yield based on 2,2′-bipyrimidine consumed) or 1-(2,2′-$C_8H_6N_4$)-1-(Me_2CH)-1-In-2-($SiMe_3$)-3-Me-2,3-$C_2B_4H_4$ (V) (0.44 g, 0.93 mmol; 68% yield based on 2,2′-bipyrimidine consumed) or the red-brown semisolid 1-(2,2′-$C_8H_6N_4$)-1-In-2-($SiMe_3$)-2,3-$C_2B_4H_5$ (VI) (0.318 g, 0.764 mmol; 79% yield based on 2,2′-bipyrimidine consumed) as the only sublimed reaction product on the inside walls of the detachable U-trap held at room temperature. Unreacted 2,2′-bipyrimidine was not identified among the products during the mild sublimation of the orange reaction residue; however, unreacted indacarborane (0.22 g, 0.58 mmol; 0.52 g, 1.65 mmol; 0.32 g, 1.05 mmol when R = $SiMe_3$, Me, H, respectively) was recovered in a trap held at −23 °C. The side arms of both the reaction flask and the U-trap were maintained at 150–160 °C by means of a heating pipe tape during the sublimation. A small quantity of a dark brown residue that remained in the reaction flask after sublimation was found to be insoluble in organic solvents and was discarded without identification. Since the complexes IV and V have limited solubility in nonpolar organic solvents at room temperature, they were recrystallized from hot benzene.

The physical properties and characterization of these complexes are as follows: IV, mp 177–179 °C dec; V, mp 192–194 °C; VI, semisolid, slightly soluble in $CDCl_3$, C_6D_6, THF, solubility increases at higher temperature without decomposition. Mass spectral analysis (high-resolution electron impact (HREI) peak match): theoretical mass for V, $^{12}C_{17}{}^{1}H_{30}{}^{11}B_4{}^{14}N_4{}^{28}Si^{115}In$ m/e 477.1650, measured mass m/e 477.1663. Anal. Calcd for $C_{19}H_{35}Si_2B_4N_4In$ (IV): C, 42.75; H, 6.61; N, 10.50. Found: C, 44.03; H, 6.67; N, 10.66.

X-ray Analyses of the Dimeric *closo*-1-(Me_2CH)-1-In-2,3-($SiMe_3$)$_2$-2,3-$C_2B_4H_4$ (I) and the Unbridged 1-(2,2′-$C_8H_6N_4$)-1-(Me_2CH)-1-In-2,3-($SiMe_3$)$_2$-2,3-$C_2B_4H_4$ (IV). Colorless, plate-shaped crystals of I, grown from its syrupy liquid in vacuum-sealed glass tubes held at 0 °C, and yellowish, plate-shaped crystals of IV, grown from benzene solution, were mounted on a Siemens R3m/V diffractometer. Final unit-cell parameters were obtained by a least-squares fit of 24 accurately centered reflections measured in the ranges 18° ≤ 2θ ≤ 29° and 16° ≤ 2θ ≤ 28° for I and IV, respectively. The pertinent crystallographic data are summarized in Table 1. Intensity data were collected in the ranges of 3° ≤ 2θ ≤ 42° and 3° ≤ 2θ ≤ 45° for I and IV, respectively, using Mo Kα radiation at 230 K. Three standard reflections monitored after every 150 reflections did not show any significant change in intensity during the data collection. These data were corrected for Lorentz–polarization effects, and a semiempirical absorption study (ψ scans) was applied. The structures were solved by SHELXTL-PLUS[28] and subsequent difference Fourier maps. The cage hydrogen atoms of I were located in difference Fourier maps, and their positions were refined. However, the silylmethyl and the isopropyl hydrogen atoms were placed in calculated positions and were included in the refinement with fixed isotropic thermal parameters. Final full-matrix least-squares refinements were carried out using the SHELXTL-PLUS system of programs.[28] Neutral-atom scattering factors were taken from ref 29. All non-hydrogen atoms of I and IV were refined anisotropically. The unit cell of I consists of two indacarborane dimers, with each indacarborane in a dimer being crystallographically unique. Carborane-cage H atoms in IV were located from DF maps, while silylmethyl, *i*-Pr, and 2,2′-bipyrimidine H's were calculated. The final atomic coordinates are listed in Table 2, and some selected bond lengths and bond angles are presented in Table 3.

Table 1. Crystallographic Data[a] for I and IV

	I	IV
formula	$C_{22}H_{58}B_8Si_4In_2$	$C_{19}H_{35}B_4N_4Si_2In$
fw	751.2	533.7
cryst syst	triclinic	monoclinic
space group	$P\bar{1}$	$P2_1$
a, Å	11.018(3)	11.428(3)
b, Å	12.394(3)	9.802(3)
c, Å	14.485(4)	11.972(3)
α, deg	73.01(2)	
β, deg	87.67(2)	96.28(2)
γ, deg	89.90(2)	
V, Å^3	1890.0(9)	1333.0(6)
Z	2	2
D_{calcd}, g cm^{-3}	1.32	1.33
abs coeff, mm^{-1}	1.34	0.973
cryst dmns, mm	0.25 × 0.10 × 0.05	0.15 × 0.30 × 0.10
scan type	θ/2θ	θ/2θ
scan speed in ω, deg min^{-1}: min, max	6.0, 30.0	5.0, 25.0
2θ range, deg	3.0–42.0	3.0–45.0
data collected	4190	2985
T, K	230	230
decay, %	0	0
no. of obsd rflns, $I > 3.0\sigma(I)$	3444	1812
no. of params refined	325	270
GOF	1.42	1.67
R^b	0.027	0.026
R_w	0.037	0.034
$\Delta\rho_{max,min}$, e Å^{-3}	+0.41, −0.53	+0.35, −0.65
k^c	0.0004	0.0003

[a] Graphite-monochromatized Mo Kα radiation; λ = 0.710 73 Å. [b] $R = \sum||F_o| - |F_c||/\sum|F_o|$; $R_w = [\sum w(F_o - F_c)^2/\sum w(F_o)^2]^{1/2}$. [c] $w = 1/[\sigma^2(F_o) + k(F_o)^2]$.

Calculations. Molecular orbital calculations using the unparameterized Fenske–Hall method[30] were carried out on model compounds VII and VIII, which have the same relative heavy-atom positions as found in I and IV, respectively, except that the $SiMe_3$ groups on the cage carbons were replaced by hydrogen atoms. The basis functions used were generated by the numerical Xα atomic orbital program of Herman and Skillman,[31] used in conjunction with the Xα-to-Slater basis program of Bursten and Fenske.[32] The relative hydrogen positions were determined as described elsewhere.[15] A set of internal coordinates was chosen such that the pseudo mirror plane of the carborane, defined by B(4), B(6), and the midpoints of the C(1)–C(2) and B(3)–B(5) axes, was the xz plane and B(4) was on the x axis (see Figures 1 and 2 for the atom-numbering system).

Results and Discussion

Synthesis. The reaction of (*i*-Pr)InI_2 with *closo-exo*-4,5-Li(THF)-1-Na(THF)-2-($SiMe_3$)-3-R-2,3-$C_2B_4H_4$ (R =

(28) Sheldrick, G. M. *Structure Determination Software Programs*; Siemens X-ray Analytical Instrument Corp.: Madison, WI, 1991.

(29) *International Tables for X-ray Crystallography*; Kynoch Press: Birmingham, U.K., 1974; Vol. IV.

(30) Hall, M. B.; Fenske, R. F. *Inorg. Chem.* **1972**, *11*, 808.

(31) Herman, F.; Skillman, S. *Atomic Structure Calculations*; Prentice-Hall: Englewood, NJ, 1963.

(32) (a) Bursten, B. E.; Fenske, R. F. *J. Chem. Phys.* **1977**, *67*, 3138. (b) Bursten, B. E.; Jensen, R. J.; Fenske, R. F. *J. Chem. Phys.* **1978**, *68*, 3320.

Table 2. Atomic Coordinates (×10⁴) and Equivalent Isotropic Displacement Parameters (Å² × 10³)

	x	y	z	U(eq)[a]
		Compound I		
In(1)	392(1)	1736(1)	1784(1)	46(1)
In(2)	916(1)	4747(1)	1566(1)	40(1)
Si(1)	−2834(1)	24(1)	1426(1)	55(1)
Si(2)	−2709(1)	1140(1)	3669(1)	45(1)
Si(3)	2542(1)	4017(1)	4239(1)	41(1)
Si(4)	4295(1)	6126(1)	2047(1)	39(1)
C(1)	−1930(4)	1229(3)	1607(3)	40(2)
C(2)	−1898(4)	1676(3)	2455(3)	37(2)
B(3)	−1233(5)	2852(4)	2203(4)	44(2)
B(4)	−845(5)	3181(4)	1003(4)	40(2)
B(5)	−1279(5)	2031(5)	694(4)	49(2)
B(6)	−2304(5)	2624(5)	1394(4)	44(2)
C(11)	2529(4)	4176(3)	2903(3)	32(2)
C(12)	3159(4)	4992(3)	2051(3)	33(2)
B(13)	3034(5)	4654(4)	1098(4)	40(2)
B(14)	2286(5)	3383(4)	1452(4)	39(2)
B(15)	1966(5)	3156(4)	2637(4)	37(2)
B(16)	3437(5)	3612(4)	2165(4)	35(2)
C(21)	1320(5)	210(5)	2475(7)	108(4)
C(22)	669(6)	−802(5)	2561(7)	142(5)
C(23)	2563(6)	259(6)	2575(6)	112(4)
C(24)	−2077(8)	−447(6)	447(5)	121(4)
C(25)	−2946(5)	−1251(4)	2494(4)	64(2)
C(26)	−4391(6)	515(5)	1054(5)	97(3)
C(27)	−1877(5)	−92(4)	4414(4)	69(2)
C(28)	−2690(6)	2237(5)	4306(4)	79(3)
C(29)	−4342(5)	778(5)	3595(4)	68(2)
C(31)	−297(4)	6041(4)	1753(3)	47(2)
C(32)	−1504(5)	6015(5)	1328(4)	64(2)
C(33)	−400(6)	6017(5)	2796(4)	86(3)
C(34)	1052(5)	3380(4)	4783(3)	60(2)
C(35)	2656(5)	5371(4)	4552(4)	64(2)
C(36)	3788(5)	3056(4)	4788(3)	60(2)
C(37)	5130(5)	6595(4)	857(3)	57(2)
C(38)	3472(5)	7377(4)	2214(5)	72(3)
C(39)	5446(4)	5581(4)	2974(4)	58(2)
		Compound IV		
In	118(1)	0	7957(1)	39(1)
Si(1)	−2734(1)	−2993(2)	7292(1)	44(1)
Si(2)	−3657(1)	669(2)	6396(1)	42(1)
C(1)	−2121(5)	−1303(6)	7829(5)	35(2)
C(2)	−2409(4)	97(8)	7443(4)	33(1)
B(3)	−1755(6)	1180(7)	8235(6)	37(2)
B(4)	−1047(5)	299(6)	9335(5)	37(2)
B(5)	−1283(5)	−1343(7)	8958(6)	39(2)
B(6)	−2460(5)	−189(8)	8832(5)	37(2)
C(21)	576(7)	−647(11)	6354(6)	92(4)
C(22)	1569(10)	−1246(22)	6254(10)	237(13)
C(23)	44(11)	111(28)	5435(8)	229(12)
C(24)	−4092(6)	−3496(8)	7925(7)	71(3)
C(25)	−3028(6)	−3034(9)	5714(5)	70(3)
C(26)	−1594(6)	−4319(8)	7656(7)	75(3)
C(27)	−3996(7)	2492(8)	6634(7)	89(3)
C(28)	−5056(4)	−293(7)	6537(5)	54(2)
C(29)	−3305(6)	556(10)	4910(5)	74(3)
N(31)	1369(3)	2003(5)	8099(4)	41(1)
C(32)	1030(5)	3247(7)	7735(5)	53(2)
C(33)	1778(6)	4288(8)	7705(6)	63(2)
C(34)	2940(6)	4050(8)	8102(6)	65(3)
N(35)	3314(4)	2838(6)	8500(5)	54(2)
C(36)	2509(4)	1868(6)	8488(4)	37(2)
N(37)	1999(4)	−400(5)	8988(4)	40(2)
C(38)	2292(5)	−1609(8)	9457(5)	57(2)
C(39)	3435(5)	−1906(8)	9839(5)	57(2)
C(40)	4242(5)	−936(8)	9738(6)	55(2)
N(41)	3983(4)	298(6)	9306(4)	48(2)
C(42)	2868(5)	499(6)	8954(4)	40(2)

[a] Equivalent isotropic U, defined as one-third of the trace of the orthogonalized U_{ij} tensor.

$SiMe_3$, Me, H) in a molar ratio of 1:1 in THF solution produced *closo*-1-(Me_2CH)-1-In-2,3-($SiMe_3$)$_2$-2,3-$C_2B_4H_4$ (**I**), *closo*-1-(Me_2CH)-1-In-2-($SiMe_3$)-3-Me-2,3-$C_2B_4H_4$ (**II**) and *closo*-1-(Me_2CH)-1-In-2-($SiMe_3$)-2,3-$C_2B_4H_5$ (**III**) as air-sensitive colorless oily liquids in 39, 36, and 27% yields, respectively, as shown in Scheme 1.

The reaction between *closo*-indacarborane and 2,2′-bipyrimidine in a molar ratio of 2:1 in benzene was instantaneous and produced the 1:1 donor–acceptor complexes 1-(2,2′-$C_8H_6N_4$)-1-(Me_2CH)-1-In-2,3-($SiMe_3$)$_2$-2,3-$C_2B_4H_4$ (**IV**), 1-(2,2′-$C_8H_6N_4$)-1-(Me_2CH)-1-In-2-($SiMe_3$)-3-Me-2,3-$C_2B_4H_4$ (**V**), and 1,1′-(2,2′-$C_8H_6N_4$)-1-(Me_2CH)-1-In-2-($SiMe_3$)-2,3-$C_2B_4H_5$ (**VI**) in 68–91% yields. The reactivity of *closo*-indacarborane toward the Lewis base is similar to that of *closo*-germacarborane[8] in that only 1:1 adducts are formed, as opposed to the *closo*-galla-,[14] *closo*-stanna-,[3] or *closo*-plumbacarboranes,[8] in which 2:1 adducts can be produced. Even with an excess of the indacarborane there was no hint of the formation of the bimetallacarborane bridged complex. It is not known whether the 2:1 complex failed to be formed in the original reaction mixture or whether it was destroyed in the purification procedure. However, it does indicate that the indacarboranes form weaker complexes with bipyrimidine than do the gallacarboranes.

Characterization. The *closo*-indacarboranes **I–III** and their donor–acceptor complexes **IV–VI** were characterized on the basis of ^1H, ^{11}B, and ^{13}C pulse Fourier transform NMR (Table 4) and IR (Table 5) spectra. Complexes **I** and **V** were further characterized by mass spectrometry and **I** and **IV** by single-crystal X-ray analyses (Tables 1–3). The high-resolution electron impact (HREI) mass spectra and the isotope patterns of the *closo*-indacarborane **I** and the 2,2′-bipyrimidine adduct **V** are consistent with their molecular formulas. The elemental analyses of **I–IV** gave results that confirmed their formulas as given in the Experimental Section. The formula of **VI** is based on the similarities between its spectral properties and preparative route and those of the more fully characterized bipyrimidine complexes **IV** and **V**.

NMR and IR Spectra. The ^1H NMR and ^{13}C NMR spectra indicate the presence of a C_2B_4 carborane cage, isopropyl, $SiMe_3$, and Me or CH groups in compounds **I-VI**, and the presence of a 2,2′-bipyrimidine ligand in each of the donor–acceptor complexes **IV-VI** (See Table 4). The ^{11}B NMR spectra of all the indacarboranes (**I-VI**) show generally the same pattern, that is, basal boron (other than the unique) resonances in the 10–16 ppm region, unique boron resonances in the 0–10 ppm region, and apical boron resonances around −40 to −50 ppm. This pattern is a typical one for metallacarboranes derived from the carborane ligands used in this study. The chemical shifts of the apical borons in these metallacarboranes have been shown to be very sensitive to the nature of the capping metal group. The apical boron resonances of the [2-($SiMe_3$)-3-R-2,3-$C_2B_4H_4$]$^{2-}$ precursors are at −44.53, −48.16, and −47.74 ppm for R = $SiMe_3$, Me, and H, respectively.[33] Comparison of these values with the ones listed in Table 4 shows that coordination of the dianions by an i-$PrIn^{2+}$ group causes a small downfield shift of the apical boron resonance of about 4 ppm; such downfield shifts normally accompany the formation of other metallacarboranes in the C_2B_4 carborane system. The explanation offered for these shifts is that the apical boron and the capping metal compete for the same π-type electrons in the C_2B_3 face of the carborane and that any

(33) Hosmane, N. S.; Saxena, A. K.; Barreto, R. D.; Zhang, H.; Maguire, J. A.; Jia, L.; Wang, Y.; Oki, A. R.; Grover, K. V.; Whitten, S. J.; Dawson, K.; Tolle, M. A.; Siriwardane, U.; Demisse, T.; Fagner, J. S. *Organometallics* **1993**, *12*, 3001.

Table 3. Selected Bond Lengths (Å) and Bond Angles (deg)[a]

Bond Lengths							
Compound I							
In(1)–Cnt(1)	2.100	In(1)–C(1)	2.676(5)	B(3)–B(6)	1.775(8)	B(4)–B(5)	1.688(9)
In(1)–C(2)	2.660(4)	In(1)–B(3)	2.425(6)	B(4)–B(6)	1.756(7)	B(5)–B(6)	1.784(9)
In(1)–B(4)	2.297(5)	In(1)–B(5)	2.431(6)	C(11)–C(12)	1.494(5)	C(11)–B(15)	1.561(7)
In(1)–B(14)	2.847(5)	In(1)–B(15)	3.014(6)	C(11)–B(16)	1.727(7)	C(12)–B(13)	1.566(8)
In(1)–C(21)	2.143(6)	In(2)–Cnt(2)	2.083	C(12)–B(16)	1.697(7)	B(13)–B(14)	1.710(7)
In(2)–B(3)	3.248(5)	In(2)–B(4)	3.045(6)	B(13)–B(16)	1.772(7)	B(14)–B(15)	1.679(8)
In(2)–C(11)	2.624(4)	In(2)–C(12)	2.639(4)	B(14)–B(16)	1.743(8)	B(15)–B(16)	1.761(7)
In(2)–B(13)	2.416(5)	In(2)–B(14)	2.302(5)	C(21)–C(22)	1.417(9)	C(21)–C(23)	1.386(9)
In(2)–B(15)	2.446(5)	In(2)–C(31)	2.156(5)	C(31)–C(32)	1.493(7)	C(31)–C(33)	1.501(8)
C(1)–C(2)	1.490(7)	C(1)–B(5)	1.551(6)	In(1)–H(14)	2.48	In(1)–H(15)	2.79
C(1)–B(6)	1.717(7)	C(2)–B(3)	1.570(7)	In(2)–H(3)	3.11	In(2)–H(4)	2.53
C(2)–B(6)	1.714(6)	B(3)–B(4)	1.702(8)				
Compound IV							
In–Cnt(3)	2.219	In–C(1)	2.849(6)	C(1)–B(5)	1.569(8)	C(1)–B(6)	1.698(9)
In–C(2)	2.888(4)	In–B(3)	2.487(7)	C(2)–B(3)	1.559(9)	C(2)–B(6)	1.694(7)
In–B(4)	2.250(6)	In–B(5)	2.480(7)	B(3)–B(4)	1.703(9)	B(3)–B(6)	1.757(10)
In–C(21)	2.141(8)	In–N(31)	2.424(5)	B(4)–B(5)	1.685(9)	B(4)–B(6)	1.728(7)
In–N(37)	2.391(4)	C(1)–C(2)	1.474(10)	B(5)–B(6)	1.751(9)		
Bond Angles							
Compound I							
Cnt(1)–In(1)–C(21)	134.9	Cnt(2)–In(2)–C(31)	139.1	B(4)–B(6)–B(5)	57.0(3)	Si(3)–C(11)–C(12)	131.9(3)
In(1)–C(21)–C(22)	115.4(5)	In(1)–C(21)–C(23)	118.7(4)	Si(3)–C(11)–B(15)	115.0(3)	C(12)–C(11)–B(15)	112.0(4)
In(2)–C(31)–C(32)	113.5(4)	In(2)–C(31)–C(33)	110.5(3)	Si(3)–C(11)–B(16)	131.8(3)	C(12)–C(11)–B(16)	63.1(3)
Si(1)–C(1)–C(2)	130.3(3)	Si(1)–C(1)–B(5)	116.6(4)	B(15)–C(11)–B(16)	64.5(3)	Si(4)–C(12)–C(11)	128.0(3)
C(2)–C(1)–B(5)	112.1(4)	Si(1)–C(1)–B(6)	129.9(3)	Si(4)–C(12)–B(13)	118.1(3)	C(11)–C(12)–B(13)	112.5(4)
C(2)–C(1)–B(6)	64.2(3)	B(5)–C(1)–B(6)	65.9(3)	Si(4)–C(12)–B(16)	127.5(3)	C(11)–C(12)–B(16)	65.1(3)
Si(2)–C(2)–C(1)	129.1(3)	Si(2)–C(2)–B(3)	118.0(4)	B(13)–C(12)–B(16)	65.6(3)	C(12)–B(13)–B(14)	104.8(3)
C(1)–C(2)–B(3)	112.3(4)	Si(2)–C(2)–B(6)	132.1(3)	C(12)–B(13)–B(16)	60.7(3)	B(14)–B(13)–B(16)	60.0(3)
C(1)–C(2)–B(6)	64.4(3)	B(3)–C(2)–B(6)	65.3(3)	B(13)–B(14)–B(15)	104.4(4)	B(13)–B(14)–B(16)	61.8(3)
C(2)–B(3)–B(4)	105.2(4)	C(2)–B(3)–B(6)	61.3(3)	B(15)–B(14)–B(16)	61.9(3)	C(11)–B(15)–B(14)	106.1(3)
B(4)–B(3)–B(6)	60.6(3)	B(3)–B(4)–B(5)	103.8(4)	C(11)–B(15)–B(16)	62.3(3)	B(14)–B(15)–B(16)	60.8(3)
B(3)–B(4)–B(6)	61.7(3)	B(5)–B(4)–B(6)	62.4(3)	C(11)–B(16)–C(12)	51.7(2)	C(11)–B(16)–B(13)	93.3(3)
C(1)–B(5)–B(4)	106.4(4)	C(1)–B(5)–B(6)	61.5(3)	C(12)–B(16)–B(13)	53.6(3)	C(11)–B(16)–B(14)	96.7(3)
B(4)–B(5)–B(6)	60.7(3)	C(1)–B(6)–C(2)	51.5(3)	C(12)–B(16)–B(14)	98.0(3)	B(13)–B(16)–B(14)	58.2(3)
C(1)–B(6)–B(3)	93.3(3)	C(2)–B(6)–B(3)	53.4(3)	C(11)–B(16)–B(15)	53.2(3)	C(12)–B(16)–B(15)	94.2(3)
C(1)–B(6)–B(4)	96.7(4)	C(2)–B(6)–B(4)	97.1(3)	B(13)–B(16)–B(15)	98.6(3)	B(14)–B(16)–B(15)	57.3(3)
B(3)–B(6)–B(4)	57.6(3)	C(1)–B(6)–B(5)	52.6(3)	C(22)–C(21)–C(23)	123.8(6)	C(32)–C(31)–C(33)	112.7(4)
C(2)–B(6)–B(5)	92.3(3)	B(3)–B(6)–B(5)	97.1(4)				
Compound IV							
Cnt(3)–In–C(21)	119.9	Cnt(3)–In–N(31)	128.9	B(5)–B(4)–B(6)	61.7(4)	C(1)–B(5)–B(4)	105.8(5)
Cnt(3)–In–N(37)	133.8	C(21)–In–N(37)	96.9(2)	C(1)–B(5)–B(6)	61.2(4)	B(4)–B(5)–B(6)	60.4(4)
N(31)–In–N(37)	66.8(1)	Si(1)–C(1)–C(2)	130.5(4)	C(1)–B(6)–C(2)	51.5(4)	C(1)–B(6)–B(3)	93.1(4)
Si(1)–C(1)–B(5)	116.2(4)	C(2)–C(1)–B(5)	112.8(5)	C(2)–B(6)–B(3)	53.7(4)	C(1)–B(6)–B(4)	98.5(4)
Si(1)–C(1)–B(6)	134.5(4)	C(2)–C(1)–B(6)	64.1(4)	C(2)–B(6)–B(4)	99.5(4)	B(3)–B(6)–B(4)	58.5(4)
B(5)–C(1)–B(6)	64.7(4)	Si(2)–C(2)–C(1)	127.9(4)	C(1)–B(6)–B(5)	54.1(3)	C(2)–B(6)–B(5)	94.8(4)
Si(2)–C(2)–B(3)	118.8(5)	C(1)–C(2)–B(3)	111.5(4)	B(3)–B(6)–B(5)	98.4(4)	B(4)–B(6)–B(5)	57.9(3)
Si(2)–C(2)–B(6)	126.8(3)	C(1)–C(2)–B(6)	64.4(4)	In–C(21)–C(22)	121.3(7)	In–C(21)–C(23)	114.6(9)
B(3)–C(2)–B(6)	65.2(4)	C(2)–B(3)–B(4)	106.3(5)	C(22)–C(21)–C(23)	118.4(10)	In–N(31)–C(32)	124.6(3)
C(2)–B(3)–B(6)	61.1(4)	B(4)–B(3)–B(6)	59.9(4)	In–N(31)–C(36)	119.2(4)	In–N(37)–C(38)	122.1(4)
B(3)–B(4)–B(5)	103.2(4)	B(3)–B(4)–B(6)	61.6(4)	In–N(37)–C(42)	120.5(3)		

[a] Cnt(1) and Cnt(2) stand for the centroids of C_2B_3 rings in structure I; Cnt(3) denotes the centroid in structure IV.

interaction that causes, or strengthens, metal–carborane bonding will tend to draw electron density away from the apical boron, thereby deshielding it and producing a downfield shift of its ^{11}B NMR resonance. Complexation of the capping metal with another Lewis base, such as bipyrimidine, should result in the transfer of electron density back to the carborane, producing a shift back upfield.[6] An inspection of the results in Table 4 show that this is the case for the indacarboranes. The downfield shifts observed in the formation of the analogous gallacarboranes are all about 4 ppm greater than those found in the indacarboranes,[14] while those found for the group 14 metallacarboranes are greater still, with changes of between 40 and 50 ppm being observed when these metals coordinate with the carborane dianions. If the above explanation for the apical boron shifts is correct, the smaller downfield shifts found in the indacarboranes are presumably due to less carborane-to-metal electron transfer, which is indicative of a more ionic (less covalent) interaction between the indium and carborane than is found in the other group 13 and 14 metallacarboranes. Some caution should be exercised in interpreting these NMR shifts in terms of total electron density. Hermánek and co-workers have shown that specific orbital population is more important than gross electron density in determining the effect of a heteroatom, E, on the chemical shift of the antipodal borons in a series of heterocarboranes of the form *closo*-$EB_{11}H_{11}$ and EB_9H_9.[34] In this regard it should be pointed out that the chemical shift of the apical boron in IV is −51.8 ppm, which is further upfield than the vlue of −44.5 ppm for the Na/Li compound of the dianion.

The infrared spectra of I-VI (Table 5) are all consistent with the formulas proposed for these compounds. One interesting feature of the infrared spectra of I-III is the

(34) (a) Hermánek, S.; Hnyk, D.; Havlas, Z. *J. Chem. Soc., Chem. Commun.* 1989, 1859. (b) Bühl, M.; Schleyer, P. v. R.; Havlas, Z.; Hnyk, D.; Hermánek, S. *Inorg. Chem.* 1991, *30*, 3107.

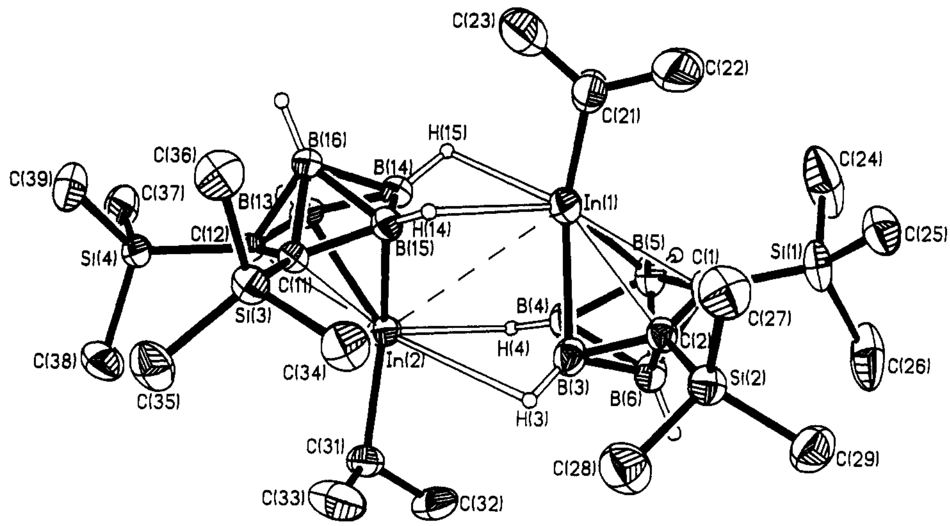

Figure 1. Perspective view of the dimeric *closo*-1-(Me_2CH)-1-In-2,3-($SiMe_3$)$_2$-2,3-$C_2B_4H_4$ (**I**) showing the atom-numbering scheme. The thermal ellipsoids are drawn at the 40% probability level. The $SiMe_3$ and the isopropyl H's are omitted for clarity.

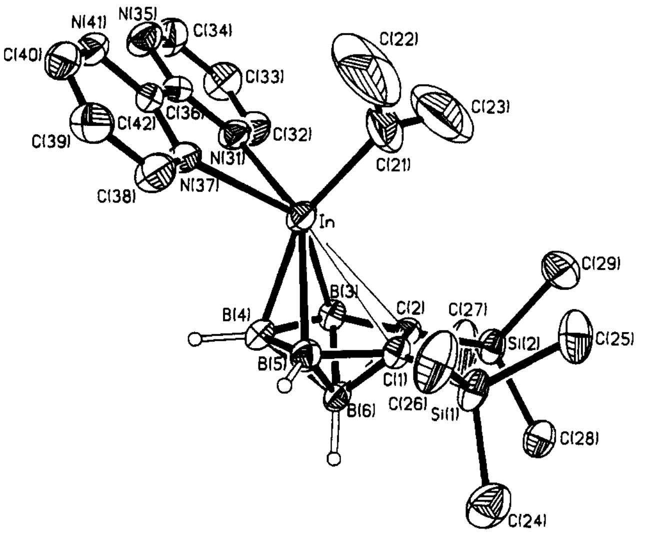

Figure 2. Perspective view of 1-(2,2′-$C_8H_6N_4$)-1-(Me_2CH)-1-In-2,3-($SiMe_3$)$_2$-2,3-$C_2B_4H_4$ (**IV**) showing the atom-numbering scheme. The thermal ellipsoids are drawn at the 40% probability level. The $SiMe_3$, the isopropyl, and the 2,2′-bipyrimidine H's are omitted for clarity.

Scheme 1

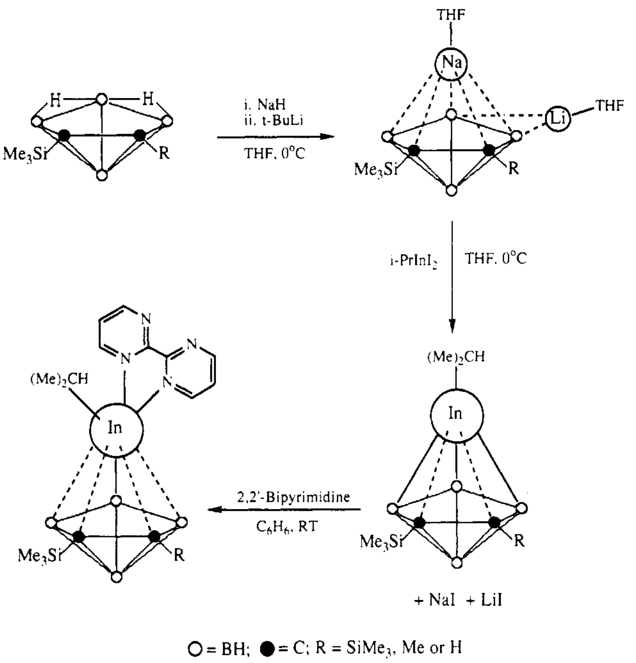

splitting of the B–H stretching modes near 2500 cm^{-1}, which is absent in their corresponding bipyrimidine complexes (**IV-VI**). Such splitting has been observed previously in a number of metallacarboranes in both the pentagonal-bipyramidal and icosahedral systems[33,35] and has been explained on the basis of ionic interactions between some of the terminal carborane hydrogens and the capping metal cation,[35b] or some exopolyhedral metal counterions.[33] The solid-state structure of **I**, shown in Figure 1, is that of a dimer in which the capping metal of one indacarborane interacts strongly with two terminal hydrogens of its neighbor within the dimeric unit. In a fairly low dielectric constant solvent, such as $CDCl_3$,[36] the solvent used in these IR studies, it is reasonable to assume that dimer formation would persist, and a splitting of the B–H stretching peaks in **I-III** would not be unexpected.

Crystal Structures of the Dimeric *closo*-1-(Me_2CH)-1-In-2,3-($SiMe_3$)$_2$-2,3-$C_2B_4H_4$ (I) and the Unbridged 1-(2,2′-$C_8H_6N_4$)-1-(Me_2CH)-1-In-2,3-($SiMe_3$)$_2$-2,3-$C_2B_4H_4$ (IV) and Molecular Orbital Analysis. Figure 1 shows the structure of the indacarborane *closo*-1-(Me_2CH)-1-In-2,3-($SiMe_3$)$_2$-2,3-$C_2B_4H_4$ (**I**), while Figure 2 shows that of its bipyrimidine complex (**IV**). Since different cage carbon substituents normally do not result in massive structural changes, these figures should also provide good qualitative descriptions of the relative cage and base heavy-atom positions in their respective Me and H derivatives, **II**, **III** and **V**, **VI**. Table 3 lists some pertinent bond distances and bond angles in **I** and **IV**.

Figure 1 shows that the *closo*-indacarboranes exists in the solid as dimers of oppositely oriented InC_2B_4 pen-

(35) (a) Manning, M. J.; Knobler, C. B.; Hawthorne, M. F. *J. Am. Chem. Soc.* **1988**, *110*, 4458. (b) Manning, M. J.; Knobler, C. B.; Khattar, R.; Hawthorne, M. F. *Inorg. Chem.* **1991**, *30*, 2009. (c) Khattar, R.; Manning, M. J.; Knobler, C. B.; Johnson, S. E.; Hawthorne, M. F. *Inorg. Chem.* **1992**, *31*, 268. (d) Khattar, R.; Knobler, C. B.; Hawthorne, M. F. *J. Am. Chem. Soc.* **1990**, *112*, 4962; *Inorg. Chem.* **1990**, *29*, 2191 and references therein. (e) Oki, A. R.; Zhang, H.; Hosmane, N. S. *Angew. Chem., Int. Ed. Engl.* **1992**, *31*, 432.

(36) ε for $CHCl_3$ is 4.80; see: Riddick, J. A.; Bunger, W. B.; Sakano, T. K. *Techniques of Chemistry: Organic Solvents, Physical Properties and Methods of Purification*, 4th ed.; Wiley: New York, 1986; Vol. II.

Table 4. FT NMR Spectral Data[a]

compd	δ splitting, assignt ($^1J(^{11}B-^1H)$ or $^1J(^{13}C-^1H)$, Hz)	rel area
	200.13-MHz ^1H NMR Data	
I	4.9–3.2 (vbr), ill-defined peak, basal H ($^1J(^{11}B-^1H)$ unresolved); 1.41, m, *i*-Pr CH, $^3J(^1H-^1H)$ = 5.7; 1.28, d, *i*-Pr Me, $^3J(^1H-^1H)$ = 5.7; 0.91, q (br), apical H (126); 0.35, s, Me_3Si	3:1:6:1:18
II	4.5–3.0 (vbr), ill-defined peak, basal H ($^1J(^{11}B-^1H)$ unresolved); 2.43, s, Me; 1.37, m, *i*-Pr CH, $^3J(^1H-^1H)$ = 5.7; 1.32, d, *i*-Pr Me, $^3J(^1H-^1H)$ = 5.5; 0.86, q (br), apical H ($^1J(^{11}B-^1H)$ unresolved); 0.28, s, Me_3Si	3:3:1:6:1:9
III	6.17, s, CH; 4.54–2.9, q(br), basal H ($^1J(^{11}B-^1H)$ unresolved); 1.38, m, *i*-Pr CH, $^3J(^1H-^1H)$ = 7.2; 1.28, d, *i*-Pr Me, $^3J(^1H-^1H)$ = 7.3; –0.28, q (br), apical H ($^1J(^{11}B-^1H)$ unresolved); 0.22, s, Me_3Si	1:3:1:6:1:9
IV	8.92, d, bpmd ring CH (4.80); 7.35, t, bpmd ring ($^3J(^1H-^1H)$ unresolved); 3.60–4.35, q, basal H ($^1J(^{11}B-^1H)$ unresolved); 1.26, d, *i*-Pr Me ($^3J(^1H-^1H)$ unresolved]; 0.91, m, *i*-Pr CH ($^3J(^1H-^1H)$ = unresolved); 0.14, s, Me_3Si; –0.11, q, apical H ($^1J(^{11}B-^1H)$ unresolved)	4:2:3:6:1:18:1
V	9.07, d, bpmd ring CH (3.97); 7.74, t, bpmd ring ($^3J(^1H-^1H)$ unresolved); 4.1–3.60, q, basal H ($^1J(^{11}B-^1H)$ unresolved); 2.41, s, Me; 0.79, d, *i*-Pr Me ($^3J(^1H-^1H)$ unresolved); 0.72, m, *i*-Pr CH ($^3J(^1H-^1H)$ unresolved); 0.24, s, Me_3Si	4:2:3:3:6:1:9
VI	9.21, d, bpmd ring CH (5.81); 8.01, t, bpmd ring (5.7); 6.24, s, cage CH; 5.24–2.84, q, basal H ($^1J(^{11}B-^1H)$ unresolved); 1.15, d, *i*-Pr Me [$^3J(^1H-^1H)$ unresolved]; 0.94, m, *i*-Pr CH ($^3J(^1H-^1H)$ unresolved); 0.23, s, Me_3Si	4:2:1:3:6:1:9
	64.21-MHz ^{11}B NMR Data[b]	
I	16.33 (vbr), ill-defined peak, basal BH (^1J(B–H) unresolved); 9.63 (vbr), ill-defined peak, basal BH (^1J(B–H) unresolved); –41.77, d (br), apical BH (125)	2:1:1
II	11.92, d (br), basal BH (^1J(B–H) unresolved); 6.39 (vbr), ill-defined peak, basal BH (^1J(B–H) unresolved); –40.18, d (br), apical BH (179.5)	2:1:1
III	11.04 (vbr), ill-defined peak, basal BH (^1J(B–H) unresolved); 6.19 (vbr), ill-defined peak, basal BH (^1J(B–H) unresolved); –44.11, d (br), apical BH (174.1)	2:1:1
IV	16.11 (vbr), ill-defined peak, basal BH (^1J(B–H) unresolved); –0.12, d (br), basal BH (143.7); –51.81, d (br), apical BH (177.8)	2:1:1
V	11.11, d (vbr), basal BH (^1J(B–H) unresolved); 2.99, d (br), basal BH (^1J(B–H) unresolved); –45.28, d (br), apical BH (150)	2:1:1
VI	10.91 (vbr), basal BH (^1J(B–H) unresolved); 6.52, vbr, basal BH (^1J(B–H) unresolved); –44.69, d (br), apical BH (172.9)	2:1:1
	50.32-MHz ^{13}C NMR Data[a,c]	
I	124.43, s (br), cage C (SiCB); 31.23, d (br), *i*-Pr CH (127.7); 22.68, q (br), *i*-Pr Me (126); 2.57, q, Me_3Si (118.6)	2:1:2:6
II	133.05, s (br), cage C (SiCB); 126.43, s (br), cage C (CCB); 27.24, d (br), *i*-Pr CH (127.2); 22.46, q, Me (129.3); 22.01, q (br), *i*-Pr Me (125.5); 2.57, q, Me_3Si (118.6)	1:1:1:1:2:3
III	117.83, s (br), cage C (SiCB); 109.11, d, cage C (HCB) (168.3); 31.12, d, (br), *i*-Pr CH (136.9); 22.64, q (br), *i*-Pr Me (126.7); –3.05, q, Me_3Si (121.8)	1:1:1:2:3
IV	161.52, s, bpmd ring, NCN; 157.85, d, bpmd ring, CH (185.7); 127.7, s (br), cage C (SiCB); 121.4, d, bpmd ring, CH (169.9); 29.38, q, *i*-Pr Me (unresolved); 22.56, d, *i*-Pr CH (unresolved); 1.39, q, Me_3Si (118.3)	2:4:2:2:2:1:6
V	157.86, s, bpmd ring, NCN; 157.55, d, bpmd ring, CH (186.6); 126.14, s (br), cage C (SiCB); 123.23, d, bpmd ring, CH (174); 118.7, s, cage C (MeCB); 22.48, q, *i*-Pr Me (120.6); 22.26, d, *i*-Pr CH (unresolved); 21.96, q, Me (135.7); 1.28, q, Me_3Si (118.8)	2:4:1:2:1:1:2:1:3
VI	158.37, d, bpmd ring, CH (188.2); 155.43, s, bpmd ring, NCN; 124.96, d, bpmd ring, CH (161.4); 119.93, s (br), cage C (SiCB); 112.1, d, cage C (HCB) (171.4); 23.03, q, *i*-Pr Me (122); 22.63, d, *i*-Pr CH (unresolved); –0.20, q, Me_3Si (118.7)	4:2:1:2:1:2:1:3

[a] $CDCl_3$ was used as solvent and as an internal standard of δ 7.24 ppm (in the ^1H NMR spectra) and δ 77.0 ppm (in the ^{13}C NMR spectra) for compounds **I–III**, **V**, and **VI**, and C_6D_6 was used as solvent and as an internal standard of δ 7.15 ppm (in the ^1H NMR spectra) and δ 128.0 ppm (in the ^{13}C NMR spectra) for compound **IV**, with a positive sign indicating a downfield shift. Legend: s = singlet, d = doublet, t = triplet, q = quartet, v = very, br = broad. [b] Shifts relative to external $BF_3 \cdot OEt_2$. [c] Since relaxations of the quaternary and the cage carbons are slower than that of a protonated C, the relative areas of these carbons could not be measured accurately. Unambiguous assignments of the apical BH's in the ^1H NMR spectra of V and VI could not be made.

tagonal-bipyramidal cages. Although the two cages are not crystallographically equivalent, they differ mainly in the relative rotational positions of the isopropyl methyl groups. Therefore, in the discussion of some of the structural characteristics of the uncoordinated indacarborane molecules, only the geometric parameters of the cage involving In(1) will be cited. In each molecule an indium, in a formal +3 oxidation state, is bonded to an isopropyl group and occupies an apical position above the C_2B_3 bonding face of the carborane. The molecule is bent such that the isopropyl groups are oriented over the cage carbons of the carboranes. The tilt angles, which are defined as the acute angles between the *i*-Pr–In bonds and the normals drawn from the particular carborane faces to their capping In atoms, are 34.4 and 28.7° for In(1) and In(2), respectively. The closest intercage heavy-atom distances are 2.847 and 3.014 Å for the In(1)–B(14) and In(1)–B(15) distances, respectively (see Table 3). Even though the neighboring carborane cage in the dimer is located to one side of the pseudo mirror plane of a InC_2B_4 cage, the In is not displaced out of this plane. Therefore, dimer formation seems to exert little geometric influence on the internal geometry of a InC_2B_4 cage. This internal geometry is such that the indiums are not symmetrically bonded to the C_2B_3 facial atoms of their respective carborane ligands but are slipped toward the boron side of the carborane face. The pertinent bond distances are In(1)–C(1,2) = 2.67 Å, In(1)–B(3,5) = 2.43 Å, and In(1)–B(4) = 2.30 Å. There are no reported In–B bond distances with which to compare these values; however, the In–C_{cage} bond distances are considerably longer than the values of 2.24, 2.37, and 2.47 Å reported for the In–C distances in the tris(cyclopentadienyl)indium(III) complex[37] and are substantially longer than the bond distance of 2.143 Å between the In and its *i*-Pr carbon (C(21) in Figure 1).

(37) Einstein, F. W. B.; Gilbert, M. M.; Tuck, D. G. *Inorg. Chem.* **1972**, *11*, 2832.

Table 5. Infrared Absorptions (cm^{-1})[a]

I	2952 (vs), 2907 (vs), 2852 (vs), 2720 (sh) [ν(C–H)], 2576 (vvs), 2433 (s, sh) [ν(B–H)], 1935 (vw, br), 1875 (vw, br), 1456 (m, s), 1406 (m, s) [$\delta(CH)_{asym}$], 1368 (m, s), 1318 (m, br), 1252 (vs) [$\delta(CH)_{sym}$], 1180 (vs), 1142 (m, s), 1114 (m, s), 1065 (m, br), 982 (m, s), 833 (vvs, br) [ρ(CH)], 728 (w, s), 690 (m, s), 651 (m, s), 624 (m, s), 624 (m, s), 530 (w, s), 491 (w, br)
II	3155 (w, s), 2955 (vvs), 2861 (vs) [ν(C–H)], 2578 (s), 2449.7 (sh) [ν(B–H)], 2250 (vs), 1796 (m, br), 1643 (w, br), 1561 (w, s), 1461 (m, s), 1384 (m, s), 1314 (m, br), 1249 (vs), 1179 (m, s), 1144 (m, s), 1097 (w, s), 1061 (w, s), 985 (w, s), 903 (vvs), 844 (vvs), 732 (vvs), 650 (vs), 626 (sh)
III	3145 (w, s), 2942 (vvs), 2856 (vs) [ν(C–H)], 2579 (vs), 2536 (vvs), 2440 (vs) [ν(B–H)], 2248 (vs), 2120 (m, s), 1793 (m, br), 1643 (w, br), 1456 (vs), 1381 (m, s), 1356 (m, s), 1248 (vs), 1188 (vs), 1146 (vs), 1072 (vs), 981 (m, s), 906 (vvs), 842 (vvs), 728 (vvs), 650 (vs), 618 (w, s)
IV	3042 (m, s), 2955 (vvs), 2912 (sh), 2900 (m, s), 2850 (m, s) [ν(C–H)], 2595 (m, br) [ν(B–H)], 2215 (vvs), 1972 (w, br), 1710 (w, s), 1650 (m, br), 1570 (vvs), 1555 (vvs), 1460 (w, s), 1405 (vvs), 1320 (m, br), 1260 (m, s), 1245 (sh), 1190 (w, s), 1145 (vs), 992 (m, s), 925 (vvs), 838 (vs), 810 (m, s), 770 (vs), 680 (m, s), 640 (m, s), 600 (w, s), 390 (w, br)
V	3155 (w, s), 3049 (w, s), 2956 (vvs), 2849 (vs) [ν(C–H)], 2543 (vs), 2486 (vvs) [ν(B–H)], 2238 (vs), 1984 (w, br), 1796 (m, br), 1461 (w, br), 1408 (vvs), 1389 (m, s), 1267 (vs), 1244 (vs), 1191 (w, s), 1144 (w, s), 1097 (m, s), 1003 (m, s), 909 (vvs), 844 (vs), 732 (vvs), 644 (vs), 616 (w, s)
VI	2958 (vvs), 2925 (vs), 2850 (vvs) [ν(C–H)], 2560 (m, s), 2500 (vs) [ν(B–H)], 2090 (m, br), 1640 (m, br), 1570 (vvs), 1547 (sh), 1465 (m, s), 1415 (vs), 1365 (m, s), 1318 (w, s), 1248 (vs), 1190 (m, s), 1150 (m, s), 1100 (w, s), 1085 (m, s), 1042 (w, br), 1015 (w, s), 982 (m, s), 865 (sh), 835 (vvs), 755 (m, s), 685 (m, s), 655 (m, s), 570 (w, s), 460 (w, s), 390 (w, s), 325 (m, s)

[a] For compounds I–III and V, $CDCl_3$ was used as solvent and reference standard, while C_6D_6 was used for IV and VI. Legend: v = very, s = strong or sharp, m = medium, w = weak, sh = shoulder, br = broad.

The large In–C_{cage} distances in I raise the question as to whether the In and cage carbons undergo any significant bonding interactions. Indium–C_2B_3 atom overlap populations for VII were calculated to be –0.0088, 0.1789, and 0.3046 for the equivalent of the C(1,2), B(3,5), and B(4) atoms, respectively. In view of the long In–C(cage) distances and small negative overlap populations, it would be better to consider the In as being η^3-bonded to the carborane. The structure of an indacarborane molecule of I is very similar to that found for the pentagonal-bipyramidal gallacarboranes, which do not form dimers.[13,14] In both metallacarboranes the metals reside in the pseudo mirror planes of the MC_2B_4 cages but are slipped toward the boron side of the carborane bonding face, and the metal-bound alkyl groups are oriented over the cage carbons. The greatest difference in the two metallacarboranes lies in the extent of the slippage of the capping metal. Metal slippage in the pentagonal-bipyramidal complexes can be conveniently measured using the parameter Δ, which is defined as the displacement (in Å) of the metal from the normal line drawn from the apical boron, B(6) in Figure 1, to the C(1)–C(2)–B(3)–B(5) plane; a positive value of Δ indicates that, compared to the apical boron, the metal is slipped toward the boron side of the carborane's bonding face.[38] The values of Δ for In(1) and In(2), shown in Figure 1, are 0.50 and 0.42 Å, respectively, which are significantly larger than the values of 0.19 and 0.20 Å found for 1-t-Bu-1-Ga-2,3-$(SiMe_3)_2$-2,3-$C_2B_4H_4$ and 1-Me-1-Ga-2,3-$C_2B_4H_6$, respectively.[13,14] Metal slip distortion is not unique to the group 13 metallacarboranes but is also found in the group 14 metallacarboranes. However, in all other metallacarboranes the extent of slippage is much less than that found in compound I. Both the large slip distortion and dimerization of the indacarboranes may be the result of increased ionic character in the metal–carborane interactions. A review of the solid-state structures of other pentagonal-bipyramidal main-group metallacarboranes shows that dimer formation is found when the capping metal is either lead or a group 1 metal, while the more covalent metallacarboranes are monomeric. In addition, the structures of those dimers are all very similar to that shown in Figure 1, that is, oppositely oriented MC_2B_4 cages. Dimer and oligomer formations have been observed for a number of In(I) and Tl(I) compounds,[17] and metal–metal bonding in the cyclopentadienyl compounds has been discussed by Janiak and Hoffmann.[16] The In–In bond distances in many of these compounds are similar to that found in I.[16] For example, the shortest In–In distance reported to date is the 3.631-Å value found in the $\{In[C_5(CH_2Ph)_5]\}_2$ dimer,[18] which is only slightly smaller than the 3.696-Å value found in I. However, the structures of the In(I) dimers are quite different from that shown in Figure 1 in that their distances of closest approach are the In(I)–In(I) distances and there seems to be little interaction between an indium in one molecule and the nonmetal group of its neighbor in the dimer. This is not the case for the dimer shown in Figure 1. The oppositely facing InC_2B_4 cages would be the preferred alignment expected for maximum dipole–dipole attraction between the metallacarborane molecules, rather than for metal–metal bonding. Unfortunately, at the Fenske–Hall level of analysis it is not possible to assess the extent to which direct In–In covalent bonding, if any, stabilizes the dimer of I. The calculations on the model compound VII and its dimer show a small overlap population between the two indiums (0.0457) and a slight decrease in the In–C_2B_3 overlap populations, from 0.9494 to 0.8542, on forming the dimer. If direct In–In interactions produce any stabilization, it would be small compared to electrostatic interactions.

Predominantly electrostatic interactions would also tend to favor a slip distortion of the metal toward the boron side of the bonding carborane face. Mulliken charge distributions in the $[C_2B_4H_6]^{2-}$ fragment of VII show that most of the negative charge is concentrated on the three facial boron atoms of the carborane; the Mulliken charges are C(1,2) = –0.135, B(6) = 0.394, B(3,5) = –0.426, and B(4) = –0.530. Therefore, purely electrostatic interactions should favor the metal occupying a position above the carborane face that is displaced toward the boron atoms. As discussed earlier, the values of the ^{11}B NMR chemical shifts of the apical borons in I–III, relative to their group 14 and lighter group 13 counterparts, are consistent with a more ionic interaction between the metal and the carborane in the indacarboranes. It should also be pointed out that the driving force for slip distortion may not necessarily be stronger metal–carborane bonding. Semiempirical MNDO molcular orbital calculations on the stan-

(38) Because in many of the metallacarboranes the C_2B_3 face of the carborane is not planar but is folded such that the unique boron is directed toward the apical boron atom, the C(1)–C(2)–B(3)–B(5) plane is used instead of the average plane of the C_2B_3 face of the carborane. For reference the values of Δ for the C_2B_3 atoms in I and IV are C(1,2) = –1.07 and –1.08 Å, B(3,5) = 0.37 and 0.37 Å, and B(4) = 1.41 and 1.42 Å, respectively.

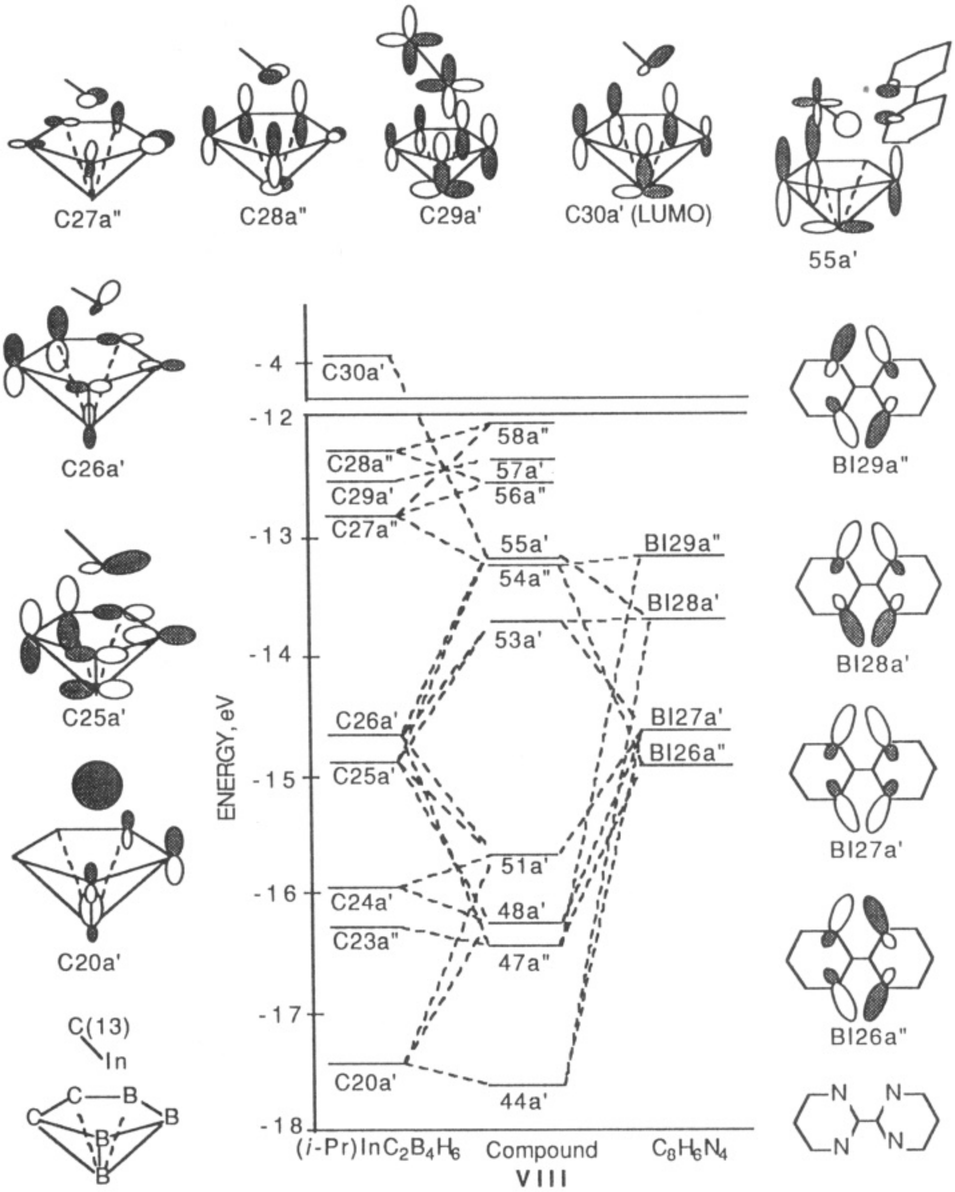

Figure 3. Molecular orbital correlation diagram of **VIII** in terms of its 1-(Me_2CH)-1,2,3-$InC_2B_4H_6$, and $C_8H_6N_4$ fragment orbitals and sketches of some of the fragment and molecular orbitals in terms of their input heavy-atom valence atomic orbitals. For clarity only the orbitals of the metal-bonding carbon of the Me_2CH group are shown.

nacarboranes showed that interactions other than tin–carborane bonding were responsible for the slip distortions in those complexes.[39]

The indacarboranes are similar to the other group 13 and 14 metallacarboranes in that they can serve as Lewis acids and form donor–acceptor complexes with Lewis bases, such as 2,2′-bipyrimidine, $C_8H_6N_4$. Figure 2 shows the structure of **IV**, the complex formed between **I** and bipyrimidine, and should also provide a good qualitative description of the structures of **V** and **VI**. The base bonds to the metallacarborane through the interactions of the base nitrogens and the capping indium metal. The structure of the resulting donor–acceptor complex is quite symmetric and closely resembles that of the corresponding bipyrimidine–gallacarborane complex.[15] The two C_4N_2 rings of the base are essentially parallel to each other, having a dihedral angle of 5.4° between them. The bipyrimidine is oriented over the boron side of the C_2B_3 carborane face and is essentially opposite the C(21) atom of the isopropyl group in the pseudo mirror plane of the metallacarborane; the dihedral angle between the pseudo mirror plane and the plane defined by C(21), In, and the midpoint of the C(36)–C(42) bond is 6.6°. The dihedral angle formed between the plane of the bipyrimidine molecule and the average C_2B_3 plane is equal to 45.2°, compared to a value of 41.0° for the bipyrimidine–gallacarborane complex.[15]

Coordination of the indium by the base induces changes in the internal indacarborane geometry. The (Me_2CH)–In tilt angle increases from around 31 to 51°, and a comparison of the analogous In–carborane bond distances in **I** and **IV**, listed in Table 3, shows that, on base coordination, the In–C(cage) bond distances increase by 0.20 Å, while the In–B(3,5) distances increase only slightly (by about 0.05 Å), with the In–B(4) distance decreasing by about the same amount. The uneven changes in bond lengths are the result of an increase in the slip distortion of the metal. The value of Δ for **IV** is equal to 0.78 Å, which is about 0.3 Å greater than that found in **I**. This is a structural change commonly found when the group 13

(39) Maguire, J. A.; Ford, G. P.; Hosmane, N. S. *Inorg. Chem.* **1988**, *27*, 3354.

and 14 carborane and cyclopentadienyl half-sandwich complexes coordinate with Lewis bases.[1,2,4,9,40] Some of the factors leading to the geometric distortions found in **IV** can be understood in terms of a molecular orbital analysis of the model compound 1-($C_8H_6N_4$)-1-(Me_2CH)-1-In-2,3-$C_2B_4H_6$ (**VIII**). Figure 3 shows the molecular orbital correlation diagram of **VIII** in terms of its $C_8H_6N_4$ and 1-(Me_2CH)-1-In-2,3-$C_2B_4H_6$ fragment orbitals (FO's). Also shown in this figure are sketches of some of the relevant fragment orbitals and complex MO's of **VIII**. Table S-4 (supplementary material) gives the composition of the filled and some of the low-energy virtual molecular orbitals (MO's) of **VIII**, in terms of their input valence atomic orbitals, and Table S-5 (supplementary material) gives the fragment orbital compositions of these MO's. As can be seen in Figure 3, the metal bonds to both the carborane and the alkyl ligands essentially through its valence *p* orbitals. The three highest energy indacarborane fragment orbitals (C27a″, C28a″, and C29a′) are localized on the boron atoms, while C25a′ and C26a′ are more heavily localized on the cage carbons. These orbitals are the ones primarily responsible for indium–carborane bonding. Figure 3 shows that FO's C27a″, C28a″, and C29a′ do not interact to any significant extent with the base; the compositions of MO's 58a″, 57a′, and 56a″ show 96%, 97%, and 96% indacarborane character, respectively. The first MO with any bipyrimidine character is MO 55a′ (43% BI28a′, 11% C30a′, 18% C26a′, and 20% C25a′), in which the indium and cage carbons are antibonding (see Figure 3). The net result is a preferential weakening of the In–C(cage) bonds that contributes to an increased slip distortion. Since the In–C_{cage} bonding in the uncomplexed indacarborane was weak to begin with, the further weakening of the bonds should not induce large additional distortions in the complex. This may be the reason that, on complexation with bipyrimidine in **IV**, Δ increases only by 0.3 Å, compared to 0.8 Å found in the gallacarborane system.[15]

The structure, reaction chemistry, and spectral properties of the indacarboranes parallel those of other main-group metallacarboranes. Those characteristic properties that do exist can qualitatively be accounted for by the assumption that the indium forms weaker, more ionic bonds with the carborane ligands than do the other group 13 and 14 metals; this would be expected from indium's position in the periodic table. Studies of the complexes of the "carbons apart" C_2B_4 carborane ligands with indium, and other metals, are currently underway in our laboratory.

Acknowledgment. This work was supported by grants from the National Science Foundation (Grant No. CHE-9100048 to N.S.H. and Grant No. CHE-9108228 to A.H.C.), the Robert A. Welch Foundation (Grant No. N-1016 to N.S.H. and Grant No. F-135 to A.H.C.), and the donors of the Petroleum Research Fund, administered by the Americal Chemical Society. Mass spectral determinations were made at the Midwest Center for Mass Spectrometry with partial support by the National Science Foundation, Biology Division (Grant No. DIR9017262).

Supplementary Material Available: Selected bond lengths and bond angles (Table S-1), anisotropic displacement parameters (Table S-2), and H atom coordinates and isotropic displacement coefficients (Table S-3) for **I** and **IV**, compositions of the molecular orbitals of **VIII** in terms of the percent atomic orbital composition (Table S-4), and fragment orbital compositions of the molecular orbitals of **VIII** (Table S-5) (36 pages). Ordering information is given on any current masthead page.

OM930476+

(40) Kohl, F. X.; Schlüter, E.; Jutzi, P.; Krüger, C.; Wolmershäuser, G.; Hofmann, P.; Stäuffert, P. *Chem. Ber.* 1984, *26*, 217.